Cr²⁺ distribution in ZnSe crystals grown from melt

D.S. Denisenko *, A.V. Timonina, T.N. Fursova, N.N. Kolesnikov

Institute of Solid State Physics RAS, Chernogolovka, 142432, MO, Russia

ARTICLE INFO

ABSTRACT

ZnSe : Cr²⁺ crystals were grown using a high-pressure vertical zone melting technique with concentrations of $5 \cdot 10^{17}$, 10^{18}, and 10^{19} cm⁻³. Infrared transmittance measurements showed a noticeable change in the Cr²⁺ ions distribution along the as-grown crystals. The effective segregation coefficients of Cr²⁺ ions were calculated and their dependence on concentration was approximated.

1. Introduction

Near-to-mid infrared lasers are of great interest for a number of applications [1] including environmental monitoring, medicine, security systems etc. Transition metal-doped $A^{II}B^{VI}$ semiconductors present great potential as active media for such lasers and show greater efficiency and tunability as compared with most sources available today [2]. Crystal growth from melt presents a problem of a dopant concentration gradient in a grown crystal.

The goal of the present study was to obtain the effective segregation coefficients of Cr²⁺ ions in ZnSe crystals grown from the melt using a high-pressure vertical zone melting (HPVZM) technique and their dependence on the initial concentration, which will be very valuable to improve the dopant concentration gradient.

2. Crystal growth and processing

ZnSe:Cr²⁺ crystals were grown by HPVZM [3] from graphite crucibles (Fig. 1) at 1540 °C under a pressure of 18 atm in the argon atmosphere at ISSP RAS autoclave using high-purity ZnSe (99.999%). The autoclave consists of a moving rod, a crucible sitting atop of it, and a heating element, all made of graphite in an evacuable chamber with a water-cooling thermo-insulated encasing.

CrSe was chosen as the source of Cr²⁺ ions. It was synthesized from raw chromium (99.995%) and selenium (99.999%) in an evacuated quartz ampoule at 1000 °C.

CrSe was placed in the seed chamber of the crucible, and ZnSe was loaded above it. The zone movement rate was 3.5 mm h⁻¹ for all crystals. The initial doping concentrations during growth were $5 \cdot 10^{17}$,

10^{18}, and 10^{19} cm⁻³. The parameters of the grown crystals are shown in Table 1.

The crystals were cut into 4-, 2- and 0.3-mm-thick plates, respectively, perpendicular to the growth direction, ground, and optically polished (Fig. 2).

3. Measurements and results

3.1. Dislocation density

To determine whether chromium ions segregate on dislocations, a sample from the top part of a crystal with $c_{Cr^{2+}} = 5 \cdot 10^{17}$ cm⁻³ was selected. Its [110] plane was etched in a 5% solution of bromine in methanol for 2 min to reveal dislocations (Fig. 3) and examined under a microscope. Examination showed etch pit density of 10^6 cm⁻² and no visible signs of decoration by chromium at ×400 optical magnification.

3.2. Dependence of the absorption coefficient on the concentration of chromium

To calculate the dependence of the effective segregation coefficient k on the concentration of Cr²⁺ ions c through the absorption coefficient β, a dependence of β on c was required.

To determine the dependence, six samples were selected from top parts of the crystals, obtained here, as well as from several previously grown. They were analyzed by inductively coupled plasma mass spectrometry (ICP-MS) and the transmission spectra of each crystal were

* Correspondence to: Shkol'nyy Bul'var, 1B, Chernogolovka, Moskovskaya oblast', 142432, Russia.
    E-mail address: DmitryAvenicci@gmail.com (D.S. Denisenko).

Seed (CrSe+ZnSe) chamber   Load (ZnSe) chamber

Graphite body   10 mm

Fig. 1. A crucible used for growth. A vertical section.

10 mm

(a) $c_{Cr2+} = 5 \cdot 10^{17}$ cm^{-3}
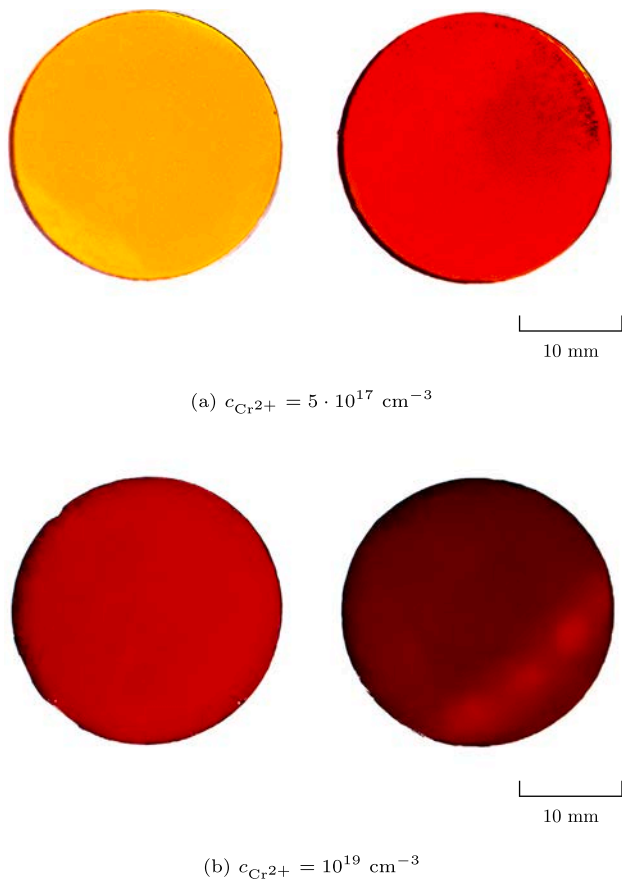

10 mm

(b) $c_{Cr2+} = 10^{19}$ cm^{-3}

Fig. 2. Samples after polishing taken from the bottom (left) and the top of a crystal (right). Note the color difference in the samples – it changes to a deep dark red as the Cr^{2+} concentration grows. (For interpretation of the references to color in this figure legend, the reader is referred to the web version of this article.)
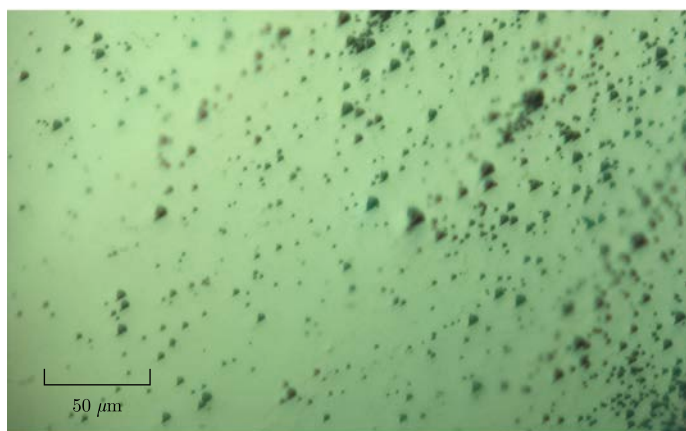

50 μm

Fig. 3. Microscopic image of the etched surface.

Table 1
Parameters of the grown crystals.

$c_{Cr^{2+}}$, cm^{-3}	$5 \cdot 10^{17}$	10^{18}	10^{19}
Length, mm	89	77	62.5
Diameter, mm	28	28	28
Weight, g	254.5	218	176
Growth rate, mm h^{-1}	3.5	3.5	3.5

Table 2
Results of the concentration analysis in the samples and the calculated absorbance.

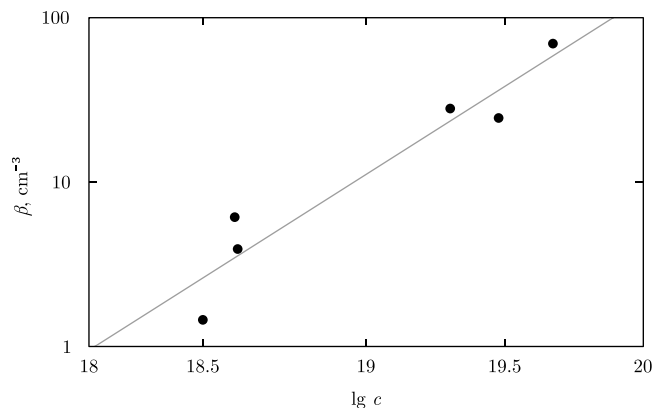| Sample	1	2	3	4	5	6
$c_{Cr^{2+}}$, $\frac{cm^{-3}}{10^{19}}$	0.34	2.02	0.26	0.34	4.75	3.02
β, cm^{-1}	3.90	27.98	1.46	6.10	69.34	24.39

Fig. 4. Dependence of the absorption coefficient β on the concentration c of Cr^{2+} ions.

measured on an Agilent Cary 5000 spectrophotometer in the range of 3300–350 nm. Obtained parameters are listed in Table 2.

Knowing the actual concentration c in each sample and respective absorption coefficient β the dependence was determined. The dependence turned out to be linear which allowed us to use absorption coefficient β in calculations instead of concentration c because transmission spectra are much easier to obtain.

The resulting dependence was approximated as

$$\beta = 4.8762c^{1.0715} \cdot 10^{-20}$$

and shown in Fig. 4.

3.3. Dependence of the effective segregation coefficient on the initial concentration of chromium

The distribution of Cr^{2+} was estimated from the optical transmission in the cut samples. The transmission spectra of each plate of three ZnSe:Cr^{2+} crystals were measured on an Agilent Cary 5000 spectrophotometer in the range of 3300–350 nm. All samples showed a clear absorption peak in the 1770 ± 3 nm region corresponding to the absorption of Cr^{2+} ions. Fig. 5 demonstrates the transmission spectra of the samples with the highest concentrations of Cr^{2+} ions from each crystal.

The slope of the spectra could be attributed to scattering on the bubbles (voids) captured by the ingots during growth [3]. The bubbles do not contribute to the ZnSe absorption [4], and the analysis of the samples with and without such defects showed no effect of defects on the value of the absorption coefficients.

Although the wurtzite–zincblende phase transition in ZnSe 100° below the melting point leads to high twinning probability, it does not contribute to distribution when using HPVZM under the assumption that no diffusion occurs in solid phases after they are formed. It is also supported by previous works [3].
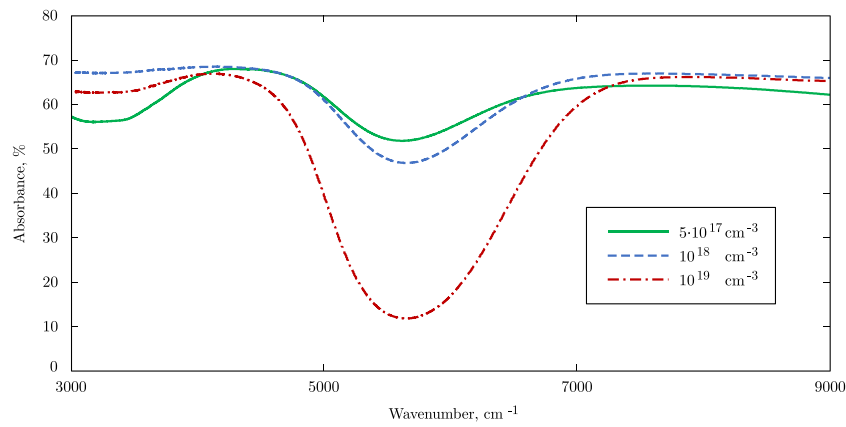
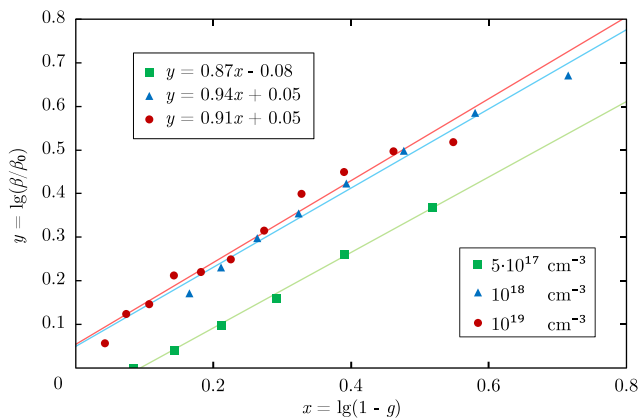**Fig. 5.** Absorption spectra of the samples from each crystal.

Fig. 6. The distribution of absorption coefficient β in the obtained crystals where g is the crystallized fraction of a crystal.

Fig. 7. Dependence of the effective segregation coefficient k on the concentration c of Cr^{2+} ions.

Using the Beer–Lambert law:

$$I(l) = I_0 e^{-\beta l},$$

the absorption coefficients β were calculated for each sample. The distribution of Cr^{2+} ions in the $ZnSe:Cr^{2+}$ ingots turned out to change noticeably along the growth direction, with β changing by several times from the bottom part of the crystal to the top (Fig. 6).

Sheil equation can be applied to HPVZM to calculate effective segregation coefficient under following assumptions [5]:

- No diffusion occurs in solid phases once they are formed $D_S = 0$
- Infinitely fast diffusion occurs in the liquid at all temperatures $D_L = \infty$
- Equilibrium exists at the solid–liquid interface, and so compositions from the phase diagram are valid
- Solidus and liquidus are straight segments.

Using the Scheil equation [6]:

$$C = kC_0(1-g)^{k-1},$$

the effective segregation coefficients k were calculated [5] for each crystal. The calculated effective segregation coefficients of Cr^{2+} ions are determined as 0.1351, 0.0901, and 0.0594 for concentrations of $5 \cdot 10^{17}$, 10^{18}, and 10^{19} cm^{-3}, respectively.

The dependence of the effective segregation coefficient k on the concentration of Cr^{2+} was approximated (Fig. 7) as
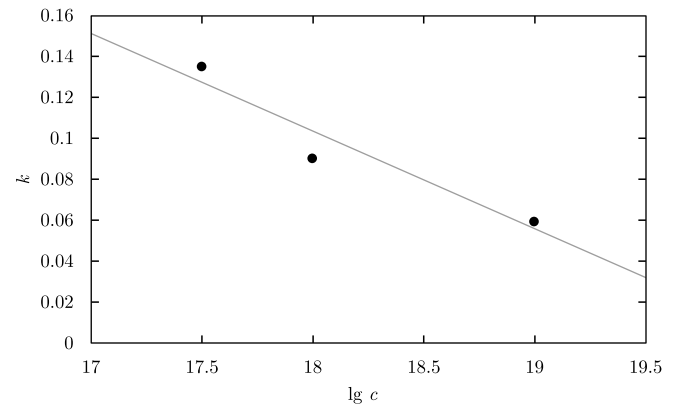
$$\beta = -0.0476 \lg c + 0.9604.$$

4. Conclusion

In the course of this work, the effective segregation coefficients have been experimentally determined for $ZnSe:Cr^{2+}$ crystals with Cr^{2+} concentrations of $5 \cdot 10^{17}$, 10^{18}, and 10^{19} cm^{-3}. The dependence of the effective segregation coefficient on the concentration of chromium under the same growth conditions has been determined. This study allows obtaining crystals with a preset final dopant concentration for a given load and with a high dopant concentration in general.

CRediT authorship contribution statement

D.S. Denisenko: Formal analysis, Investigation, Writing – original draft, Writing – review & editing, Visualization. **A.V. Timonina:** Resources, Data curation. **T.N. Fursova:** Resources, Software, Data curation. **N.N. Kolesnikov:** Conceptualization, Methodology, Validation, Resources, Data curation, Supervision, Project administration, Funding acquisition.

Declaration of competing interest

The authors declare that they have no known competing financial interests or personal relationships that could have appeared to influence the work reported in this paper.

Data availability

Data will be made available on request.

Acknowledgments

References

[1] V. Levchenko, V. Yakimovich, L. Postnova, V. Konstantinov, V. Mikhailov, N. Kuleshov, Preparation and properties of bulk ZnSe:Cr single crystals, J. Cryst. Growth 198–199 (1999) 980–983, http://dx.doi.org/10.1016/S0022-0248(98)01098-7.

[2] A. Burger, K. Chattopadhyay, J.-O. Ndap, X. Ma, S. Morgan, C. Rablau, C.-H. Su, S. Feth, R.H. Page, K.I. Schaffers, S.A. Payne, Preparation conditions of chromium doped ZnSe and their infrared luminescence properties, J. Cryst. Growth 225 (2) (2001) 249–256, http://dx.doi.org/10.1016/S0022-0248(01)00845-4, Proceedings of the 12th American Conference on Crystal Growth and Epitaxy.

[3] N.N. Kolesnikov, R.B. James, N.S. Berzigiarova, M.P. Kulakov, HPVB- and HPVZM-shaped growth of CdZnTe, CdSe, and ZnSe crystals, in: R.B. James, L.A. Franks, A. Burger, E.M. Westbrook, R.D. Durst, E.M. Westbrook, R.D. Durst (Eds.), X-Ray and Gamma-Ray Detectors and Applications IV, Vol. 4784, SPIE, International Society for Optics and Photonics, 2003, pp. 93–104, http://dx.doi.org/10.1117/12.450814.

[4] M.P. Kulakov, N.D. Ryazanova, A.V. Fadeev, et al., Absorption coefficient of melt-grown zinc selenide, Izv. Akad. Nauk SSSR, Neorg. Mater. 21 (1985) 1462–1467.

[5] W. Pfann, Zone Melting, in: Wiley Series on the Science and Technology of Materials, Wiley, 1966.

[6] E. Scheil, Bemerkungen zur schichtkristallbildung, Int. J. Mater. Res. 34 (3) (1942) 70–72, http://dx.doi.org/10.1515/ijmr-1942-340303.